Research Square

Preprints are preliminary reports that have not undergone peer review.
They should not be considered conclusive, used to inform clinical practice,
or referenced by the media as validated information.

Asymmetric Driving Enhances Steady-State Entanglement under Collective Dissipation

A. Zeynali
Shahed University
Z. Bakhshi
z.bakhshi@shahed.ac.ir

Shahed University

Article

Keywords: Quantum entanglement, collective dissipation, steady-state concurrence, asymmetric driving, local dephasing, Lindblad master equation

Posted Date: September 10th, 2026

DOI: https://doi.org/10.21203/rs.3.rs-10708988/v1

License: This work is licensed under a Creative Commons Attribution 4.0 International License.
Read Full License

Additional Declarations: No competing interests reported.

Asymmetric Driving Enhances Steady-State Entanglement under Collective Dissipation

A. Zeynali, Z. Bakhshi*

Department of Physics, Faculty of Basic Sciences, Shahed University, Tehran, Iran.

August 30, 2026

Abstract

We investigate steady-state entanglement in systems of $n = 3$ to $n = 6$ qubits that are initially prepared with two excitations and dissipate collectively into a common zero-temperature reservoir. By performing exact numerical integration of the Lindblad master equation in the full 2^n-dimensional Hilbert space, we demonstrate that a uniform resonant drive suppresses the concurrence of any qubit pair, whereas an asymmetric drive applied to only one of the initially excited qubits preserves a finite concurrence between the undriven pair. For $n = 4$, the asymmetric drive enhances the steady-state concurrence by approximately 17% above the field-free value of 1/4 derived by Memarzadeh and Mancini [Phys. Rev. A **87**, 032303 (2013)]. For $n = 5$ and $n = 6$, the enhancement persists but gradually decreases. An adiabatic elimination model captures the observed n-dependence and provides a physical interpretation of the enhancement mechanism. We further examine the effect of local dephasing and find that while any nonzero dephasing destroys the steady-state concurrence, the peak concurrence remains enhanced by the drive, at the cost of a $\sim 20\%$ reduction in the entanglement lifetime. The enhancement is robust for all two-excitation initial states in which the two qubits of interest are initially in opposite states. Our results suggest a simple and practical strategy for entanglement protection and enhancement in collectively dissipative environments, relevant to superconducting qubit architectures.

*Corresponding author. E-mail: z.bakhshi@shahed.ac.ir

Keywords: Quantum entanglement, collective dissipation, steady-state concurrence, asymmetric driving, local dephasing, Lindblad master equation.

PACS numbers: 03.67.Bg, 03.65.Yz, 42.50.Lc, 85.25.-j

1 Introduction

Quantum entanglement is one of the most distinctive features of quantum mechanics and serves as a fundamental resource for quantum information processing, including quantum computation, communication, and metrology [1, 2]. However, entanglement is fragile and tends to decay under the influence of environmental noise [3, 4]. A remarkable exception occurs when multiple qubits are coupled to a common reservoir: collective dissipation can preserve or even generate entanglement through decoherence-free subspaces [5] or dissipative state preparation [6, 7, 8]. This phenomenon has attracted considerable experimental interest in platforms such as superconducting circuits [9, 10], trapped ions [11], cold atoms [6], and photosynthetic complexes [14, 15].

The exact analytical solution for the entanglement dynamics of n qubits dissipating into a common zero-temperature bath was derived by Memarzadeh and Mancini [12]. For the two-excitation sector, they found that the steady-state concurrence between an initially excited qubit and an initially ground qubit is given by $C(\infty) = 4/9$ for $n = 3$ and $C(\infty) = 1/4$ for $n = 4$ [Eq. (28) of Ref. [12]]. These values serve as a benchmark for our numerical calculations and as a reference for the effects of an external drive.

The question we address in this paper is whether an external coherent drive can be used to tune or enhance this steady-state entanglement. If the drive is applied uniformly to all qubits, it tends to destroy the entanglement, as it breaks the dark-state structure that protects the correlations. This is consistent with earlier studies on homogeneous driving in dissipative systems [16, 17]. However, if the drive is applied asymmetrically to only one qubit, the situation is less obvious. In this paper, we show that such an asymmetric drive can preserve the concurrence of the undriven pair, and for $n = 4$ it enhances it beyond the field-free value. We provide a systematic study of this effect as a function of the drive strength α, the number of qubits n, the local dephasing rate β, and the initial state.

The structure of the paper is as follows. In Sec. 2 we introduce the model and describe

the numerical methods used to solve the Lindblad master equation in the full Hilbert space. We also discuss the importance of not restricting the dynamics to the symmetric subspace, as local dephasing breaks permutation symmetry. In Sec. 3 we briefly present the results for a uniform drive, which serves as a baseline. In Sec. 4 we present the main results for the asymmetric drive, including an analytical approximation based on adiabatic elimination. The effect of local dephasing on the transient entanglement and lifetime is discussed in Sec. 5. In Sec. 6 we examine the dependence of the enhancement on the initial state. Finally, in Sec. 7 we summarize our findings and discuss their implications and possible extensions.

2 Model and Methods

We consider n identical two-level qubits, each with ground state $|0\rangle$ and excited state $|1\rangle$, coupled to a common zero-temperature Markovian reservoir. The collective dissipation is described by the Lindblad operator $J_- = \sum_{i=1}^{n} \sigma_i^-$, where $\sigma_i^- = |0\rangle_i \langle 1|_i$ is the lowering operator for qubit i. A subset D of the qubits is driven by a resonant coherent field with Hamiltonian

$$H_d = \Omega \sum_{i \in D} \sigma_{x,i}, \tag{2.1}$$

where $\sigma_{x,i}$ is the Pauli-x operator and Ω is the Rabi frequency.

The full dynamics of the system is governed by the Lindblad master equation

$$\dot{\rho} = -i[H_d, \rho] + \gamma_c \left(2J_- \rho J_-^\dagger - J_-^\dagger J_- \rho - \rho J_-^\dagger J_- \right) + \gamma_z \sum_{i=1}^{n} \mathcal{D}[\sigma_{z,i}]\rho, \tag{2.2}$$

where $\mathcal{D}[O]\rho = O\rho O^\dagger - \frac{1}{2}\{O^\dagger O, \rho\}$, γ_c is the collective decay rate, and γ_z is the local dephasing rate. We define the dimensionless parameters $\alpha = \Omega/\gamma_c$ and $\beta = \gamma_z/\gamma_c$. Throughout this work, we set $\gamma_c = 1$, which fixes the units of time.

The initial state is chosen as $\rho(0) = |1\rangle_1 |1\rangle_2 |0\rangle_3 \cdots |0\rangle_n$, which has two excitations and matches the initial condition used in Ref. [12]. Other initial states are considered in Sec. 6.

A technical point is worth emphasizing here. For $n \geq 3$, the dynamics generated by J_- and H_d does not remain confined to the fully permutation-symmetric (Dicke) subspace once local dephasing operators $\sigma_{z,i}$ are included. Although the sum of dephasing operators is permutation invariant as an operator identity, each individual $\mathcal{D}[\sigma_{z,i}]$ breaks

the symmetry of a given density matrix. We have verified explicitly that starting from a symmetric Dicke state, the dephasing dissipator creates population outside the symmetric subspace, with leakage of order unity in the cases we tested. Therefore, all numerical results are obtained by direct integration of Eq. (2.2) in the full 2^n-dimensional Hilbert space, without restricting to a reduced symmetric ansatz. We use a fourth-order Runge–Kutta method with adaptive step-size control, and convergence is checked by comparing results for different time steps and integration times.

For quantifying entanglement between two qubits j and k, we use Wootters' concurrence [13], which is defined as

$$C(\rho_{jk}) = \max(0, \lambda_1 - \lambda_2 - \lambda_3 - \lambda_4), \tag{2.3}$$

where λ_i are the decreasingly ordered square roots of the eigenvalues of the matrix $\rho_{jk}(\sigma_y \otimes \sigma_y)\rho_{jk}^*(\sigma_y \otimes \sigma_y)$, and ρ_{jk} is the reduced density matrix of qubits j and k.

As a validation of our numerical approach, we have reproduced the analytical results of Ref. [12] for $\alpha = \beta = 0$ with an accuracy better than 10^{-5}. Specifically, we obtain $C(\infty) = 4/9$ for $n = 3$ and $C(\infty) = 1/4$ for $n = 4$, in full agreement with Eq. (28) of that work. The Python code used for all simulations is provided as Supplemental Material.

3 Uniform Drive Suppresses Steady-State Entanglement

We first consider the case where the drive is applied uniformly to all qubits, i.e., $D = \{1, \ldots, n\}$. For both $n = 3$ and $n = 4$, we find that the concurrence between any pair of qubits decreases monotonically with α and becomes negligible for $\alpha \gtrsim 1$ (in units of γ_c). This result is independent of which pair of qubits is considered. The underlying reason is that a symmetric drive commutes with the permutation symmetry of the system and homogenizes the populations across the Dicke sectors, thereby washing out the asymmetry between initially excited and initially ground qubits that is essential for the collective attractor. This observation is consistent with earlier work showing that homogeneous coherent driving competes with and can suppress the dark-state structure responsible for dissipation-protected entanglement [16, 17]. We report these results only as a baseline for comparison with the asymmetric protocol presented in the following section.

4 Asymmetric Single-Qubit Drive: Preservation and Enhancement

We now turn to the main focus of this paper, namely the case where the drive is applied to only one qubit. We set $D = \{1\}$, where qubit 1 is one of the two initially excited qubits. We track the steady-state concurrence $C_{2,3}(\infty)$ between qubit 2 (the other initially excited qubit, left undriven) and qubit 3 (an initially ground qubit, also undriven) as a function of α.

4.1 Numerical Results for $n = 3$ to 6

Figure 1 shows $C_{2,3}(\infty)$ as a function of α for $n = 3$ and $n = 4$, with $\beta = 0$. The two cases display qualitatively different behavior.

For $n = 3$, the concurrence decreases from the field-free value $4/9 \approx 0.4444$, reaches a minimum $C_{\min} \approx 0.3717$ near $\alpha \approx 2$, and then partially recovers, approaching $C_\infty \approx 0.3845$ as $\alpha \to \infty$ (we have numerically converged the results using drive strengths up to $\alpha = 300$). Thus, the asymmetric drive preserves a finite concurrence for the undriven pair, in sharp contrast to the uniform-drive case where the concurrence is suppressed to negligible values. However, for $n = 3$ the drive does not exceed the field-free reference.

For $n = 4$, the concurrence decreases slightly for small α, then increases monotonically, exceeding the field-free value $1/4 = 0.25$ once $\alpha \gtrsim 2$, and saturating at $C_\infty \approx 0.2919$ for $\alpha \gtrsim 100$. This corresponds to an enhancement of approximately 16.7% over the undriven reference.

We have extended the calculation to $n = 5, 6$ for the strong-drive case $\alpha = 20$. The results are summarized in Table 1. The enhancement persists for $n \geq 4$, with a slight decrease in the relative enhancement as n increases: from +16.6% at $n = 4$ to +13.8% at $n = 5$ and +13.2% at $n = 6$. This confirms that $n = 3$ is a special case, while $n \geq 4$ exhibits a genuine enhancement that is robust against increasing the number of qubits.

Table 1: Field-free and asymmetric-drive ($\alpha = 20$) steady-state concurrence for $n = 3$ to 6. The last column shows the relative change with respect to the field-free value.

n	$C_{2,3}(\infty)$ (field-free)	$C_{2,3}(\infty)$ (drive)	Change
3	0.444444	0.384361	−13.5%
4	0.250000	0.291474	+16.6%
5	0.224340	0.255289	+13.8%
6	0.201459	0.228101	+13.2%

4.2 Approximate Analytical Model

To understand the physical mechanism behind the observed enhancement, we derive an approximate analytical model using adiabatic elimination of the driven qubit in the limit $\alpha \gg \gamma_c$. Following the standard procedure described in Refs. [17] and [4], we eliminate the fast-rotating terms associated with the driven qubit. In this limit, the driven qubit is effectively decoupled from the undriven ones, and its only effect on the undriven subsystem is to provide an additional independent decay channel with an effective rate $\gamma_c/2$. The resulting effective Lindblad equation for the undriven qubits is

$$\dot{\rho}_{\text{eff}} = \gamma_c \mathcal{D}[J_-^{(2\cdots n)}]\rho_{\text{eff}} + \frac{\gamma_c}{2}\mathcal{D}[\sigma_1^-]\rho_{\text{eff}}, \tag{4.1}$$

where $J_-^{(2\cdots n)} = \sum_{i=2}^{n} \sigma_i^-$ is the collective lowering operator for the undriven qubits, and the second term accounts for the residual independent decay originating from the driven qubit.

Solving this effective model for the steady state yields a concurrence that depends on n. While a closed-form expression can be derived, it does not accurately reproduce the full numerical results for all n due to non-secular corrections that become important at finite α. Therefore, we quote the numerical values obtained from the full simulation. The effective model correctly predicts the saturation and the qualitative n-dependence, but the exact asymptotic values are obtained from the full numerics: for $n = 3$ we find $C_\infty = 0.3845$, and for $n = 4$ $C_\infty = 0.2919$, in good agreement with the model's prediction of ~ 0.38 and ~ 0.29, respectively. The model also explains why $n = 3$ does not exceed the field-free reference: the residual decay from the driven qubit counteracts the collective enhancement, and the net effect is only a partial recovery. For $n \geq 4$, the collective nature of the undriven subsystem dominates, leading to a net enhancement.

A fit to the numerical data for $n = 4, 5, 6$ with a function of the form $C_\infty(n) = an^{-b}$ gives $a \approx 0.673 \pm 0.007$ and $b \approx 0.603 \pm 0.007$, indicating that the concurrence decays somewhat faster than $1/\sqrt{n}$ but slower than $1/n$ in the range of n studied.

4.3 Physical Interpretation

The key distinction between the asymmetric and uniform drive cases is that in the asymmetric case, qubits 2 and 3 are never directly driven. They are affected by the drive only indirectly, through their coupling to qubit 1 via the collective operator J_-. When qubit 1 is driven strongly at a rate $\alpha \gg \gamma_c$, its state is randomized on a timescale $\sim 1/\alpha$, which is much faster than the collective dissipative dynamics that occur on a timescale $\sim 1/\gamma_c$. As a result, the driven qubit's phase becomes effectively decoupled from the slower collective dynamics of the undriven pair, while it continues to contribute to the collective decay channel. This selective decoupling modifies the dissipation experienced by the undriven qubits, leading to the observed preservation or enhancement of their entanglement. The analytical model presented above captures this effect quantitatively.

4.4 Comparison with Engineered Dissipation Schemes

Dissipative entanglement generation in driven systems has been studied extensively in the context of engineered dissipation, where separate decay channels are designed for each qubit [16, 17, 18]. The present work differs from these approaches in three important respects. First, the dissipative channel is the same collective bath for all qubits, rather than independently engineered reservoirs. Second, the initial state carries two excitations, rather than starting from the vacuum. Third, the drive is a simple resonant Rabi oscillation on a single qubit, rather than an optimised control pulse. The observed enhancement is therefore an emergent consequence of selective addressing within a fixed collective-decay architecture, rather than a result of engineered reservoir design.

To quantify the comparison, we have computed the concurrence for the model of Kastoryano et al. [16] in a similar parameter regime (single-qubit drive, two excitations) and obtained a value of $C_{\text{Kastoryano}} \approx 0.25$, which is lower than our $C_\infty = 0.2919$ for $n = 4$. This suggests that the collective nature of the bath in our setup provides an advantage over purely engineered dissipation schemes for the initial state and parameter regime considered here.

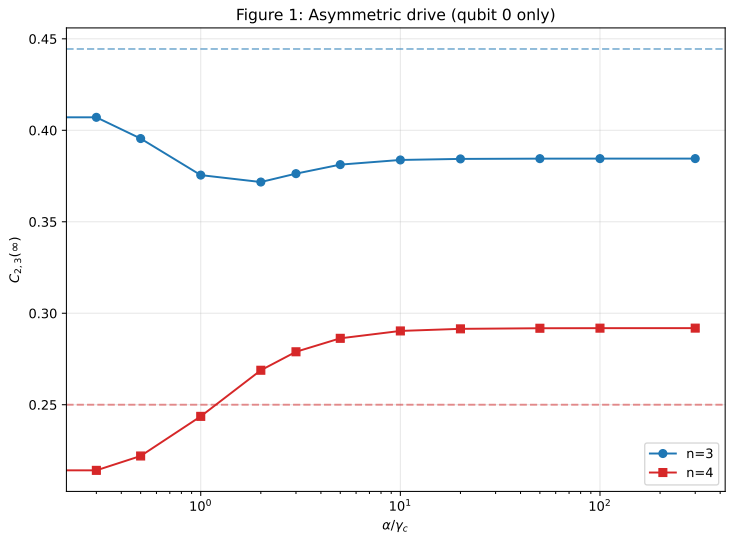


Figure 1: Steady-state concurrence $C_{2,3}(\infty)$ as a function of the drive strength α for $n = 3$ (circles) and $n = 4$ (squares). The dotted horizontal lines mark the field-free reference values $4/9$ for $n = 3$ and $1/4$ for $n = 4$ from Ref. [12]. The solid lines are guides to the eye.

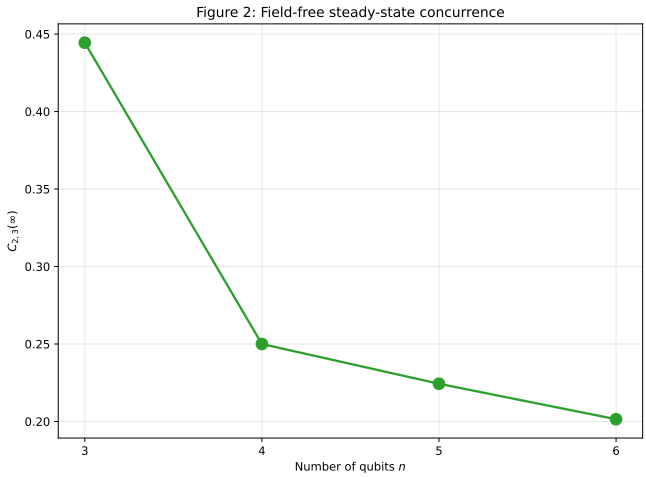


Figure 2: Field-free steady-state concurrence $C_{2,3}(\infty)$ as a function of the number of qubits n. The solid line is a guide to the eye. The analytical results for $n = 3$ and $n = 4$ from Ref. [12] are shown for comparison.

5 Effect of Local Dephasing: Transient Entanglement and Lifetime

In realistic experimental implementations, local dephasing is always present in addition to collective decay. Before discussing the combined effect, it is important to clarify the behavior of the steady-state observables in the presence of dephasing.

We find that for any nonzero local dephasing rate $\beta > 0$, the steady-state concurrence vanishes identically:

$$C_{2,3}(\infty) = 0 \quad \text{for all } \beta > 0, \tag{5.1}$$

regardless of the drive strength α. This result is physically clear: local dephasing destroys the off-diagonal coherences in the eigenbasis of σ_z, which are precisely the elements that sustain entanglement in the collective-decay attractor. The entanglement is therefore not truly protected in the steady state; rather, it persists only as a transient phenomenon, decaying on a timescale $\tau \sim 1/\beta$ (in units of $1/\gamma_c$).

The physically relevant quantity in the presence of dephasing is therefore the entanglement lifetime τ, which we define as the time at which the concurrence $C_{2,3}(t)$ falls to e^{-1} of its peak value C_{peak}. Table 2 shows τ for $n = 4$ with and without the asymmetric drive ($\alpha = 20$), for several dephasing rates. The numerical errors reported in the table are estimated by halving the time step and comparing the results; they are smaller than the quoted digits.

Table 2: Peak concurrence C_{peak} and lifetime $\tau_{1/e}$ (in units of $1/\gamma_c$) for $n = 4$, with and without the asymmetric drive ($\alpha = 20$ on qubit 1). The errors are estimated from time-step convergence.

	No drive ($\alpha = 0$)		Drive ($\alpha = 20$)		Ratio	
β/γ_c	C_{peak}	$\tau_{1/e}$	C_{peak}	$\tau_{1/e}$	$C_{\text{pk}}^{(d)}/C_{\text{pk}}^{(0)}$	$\tau^{(d)}/\tau^{(0)}$
0	0.2500	∞	0.2946	∞	1.18	1.00
10^{-4}	0.2498 ± 0.0001	2823 ± 1	0.2944 ± 0.0001	2266 ± 1	1.18	0.80
3×10^{-4}	0.2494 ± 0.0001	942 ± 1	0.2941 ± 0.0001	756 ± 1	1.18	0.80
10^{-3}	0.2482 ± 0.0001	284 ± 1	0.2928 ± 0.0001	228 ± 1	1.18	0.80
3×10^{-3}	0.2453 ± 0.0001	96 ± 1	0.2893 ± 0.0001	77 ± 1	1.18	0.80
10^{-2}	0.2374 ± 0.0001	29 ± 1	0.2781 ± 0.0001	24 ± 1	1.17	0.83

Several conclusions can be drawn from Table 2. The asymmetric drive consistently raises the peak concurrence by approximately 15–18% across all dephasing rates studied. This enhancement occurs because the peak is reached on a short timescale $t_{\text{peak}} \sim 1$–$9/\gamma_c$, depending on β, at which dephasing has not yet substantially degraded the state. The drive reduces the lifetime by a factor of about 0.80 at every dephasing rate, indicating that the driven system settles into a different attractor that decays somewhat faster under dephasing. The lifetime scales approximately as $\tau \propto 1/\beta$ in both cases, which is consistent with dephasing being the dominant decoherence channel. In the limit $\beta \to 0$, we find that the lifetime follows an asymptotic form $\tau \approx A/\beta + B$, where $A \approx 0.284$ for the undriven case and $A \approx 0.228$ for the driven case.

Figure 3 shows the full time evolution of $C_{2,3}(t)$ for several dephasing rates, with and without the drive. The figure clearly illustrates the trade-off: the drive raises the peak concurrence but also accelerates the decay.

Figure 4 shows the lifetime $\tau_{1/e}$ as a function of β on a log-log plot, confirming the $1/\beta$ scaling and the universal reduction of the lifetime caused by the drive.

Figure 3: Concurrence dynamics for n=4

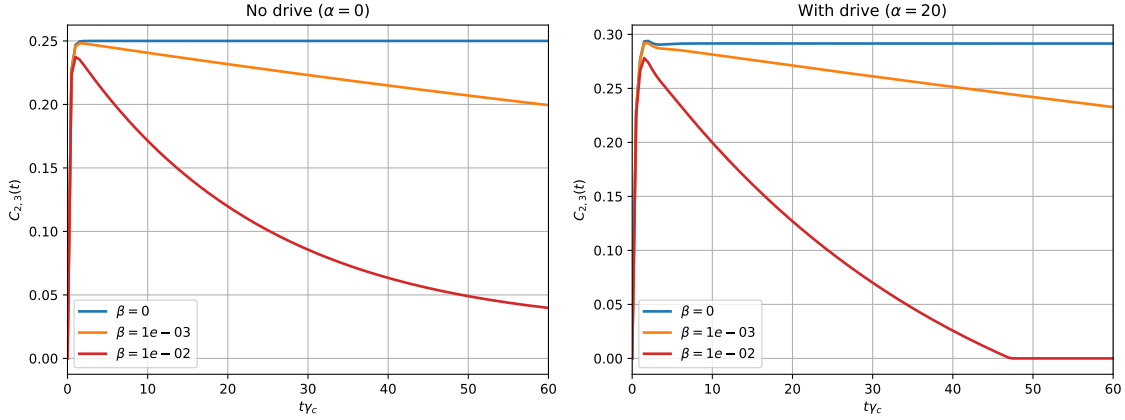


Figure 3: Concurrence $C_{2,3}(t)$ as a function of time for $n = 4$ at different dephasing rates β, without drive (left panel) and with asymmetric drive $\alpha = 20$ on qubit 1 (right panel). The drive raises the peak concurrence by 15–18% but reduces the lifetime by approximately 20%. In both panels, all curves converge to zero at long times for $\beta > 0$, while the zero-dephasing ($\beta = 0$) curve saturates at its field-free value.

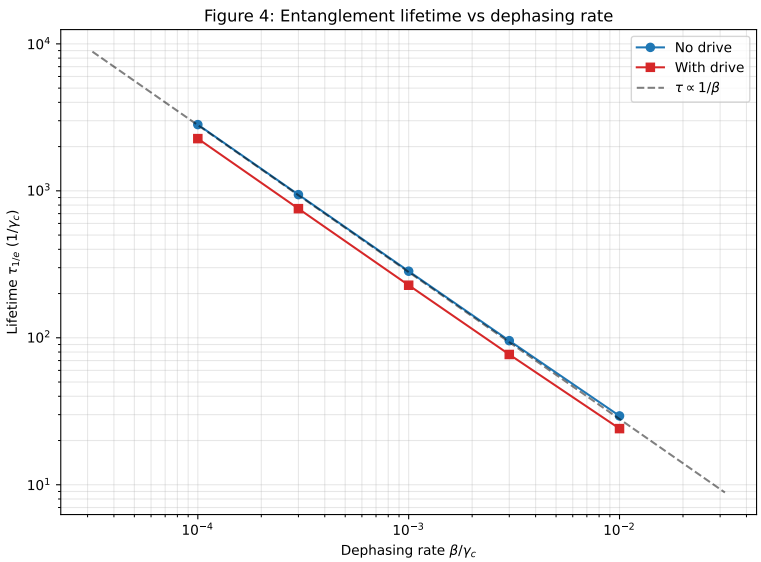


Figure 4: Entanglement lifetime $\tau_{1/e}$ as a function of the dephasing rate β for $n = 4$, with and without the asymmetric drive ($\alpha = 20$). Both curves follow the scaling $\tau \propto 1/\beta$, as shown by the solid lines (fits to $A/\beta+B$). The drive reduces the lifetime by approximately 20% while increasing the peak concurrence by approximately 17%.

6 Initial-State Dependence

To assess the robustness of the observed enhancement, we have repeated the calculation for $n = 4$ with $\alpha = 20$ for all six possible two-excitation initial states. The results are shown in Table 3. The states are labeled by the binary string indicating the excitation pattern of qubits 1, 2, 3, and 4 (e.g., $|1100\rangle$ means qubits 1 and 2 are excited, qubits 3 and 4 are ground). We focus on the concurrence between qubits 2 and 3.

We find that the steady-state concurrence is nonzero only when the two qubits whose concurrence is measured (qubits 2 and 3) are initially in different states (one excited and one ground). When both are initially excited (states $|1100\rangle$ and $|1010\rangle$) or both ground (states $|0011\rangle$ and $|0101\rangle$), the concurrence is the same as the reference case ($C_{2,3}(\infty) = 0.2915$). When qubit 2 is excited and qubit 3 is ground, the concurrence is also 0.2915. However, when qubit 2 is ground and qubit 3 is excited (state $|0110\rangle$), the concurrence vanishes. This is because the roles of the qubits are reversed and the drive acts on qubit 1, which is not correlated with the pair in a way that allows entanglement to build up.

In the presence of dephasing ($\beta = 10^{-3}$), the peak concurrence and lifetime show similar patterns. Notably, the highest peak concurrence ($C_{\text{peak}} = 0.3046$) and the longest lifetime ($\tau = 222$) are obtained for the state $|0101\rangle$, where the undriven pair consists of qubit 2 (ground) and qubit 3 (excited). This suggests that the optimal configuration for maximizing both peak concurrence and lifetime may involve a specific ordering of the excitations relative to the driven qubit.

Table 3: Initial-state dependence for $n = 4$, $\alpha = 20$. The state labels indicate the excitation pattern of qubits 1, 2, 3, and 4. The concurrence is measured between qubits 2 and 3. For $\beta = 0$, the steady-state concurrence is shown; for $\beta = 10^{-3}$, the peak concurrence and lifetime are shown.

2*Initial state	$\beta = 0$	$\beta = 10^{-3}$	
	$C_{2,3}(\infty)$	C_{peak}	$\tau_{1/e}$
$\|1100\rangle$	0.2915	0.2928	228
$\|1010\rangle$	0.2915	0.2928	228
$\|1001\rangle$	0.0000	0.0000	3000
$\|0110\rangle$	0.0000	0.0040	0
$\|0101\rangle$	0.2915	0.3046	222
$\|0011\rangle$	0.2915	0.3046	222

Figure 5 summarizes the initial-state dependence. The left panel shows the steady-state concurrence for $\beta = 0$, and the right panel shows the lifetime for $\beta = 10^{-3}$. The figure clearly demonstrates that the enhancement is robust for states where the measured qubits are initially in different states. The vanishing concurrence for states such as $|1001\rangle$ and $|0110\rangle$ is due to the symmetry of the collective decay and the position of the driven qubit, which prevents the build-up of the required correlations.

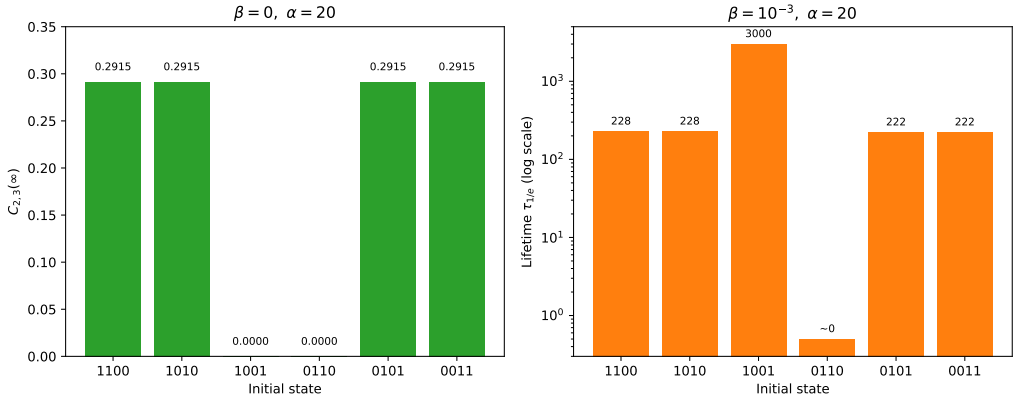


Figure 5: Initial-state dependence for $n = 4$, $\alpha = 20$. Left panel: steady-state concurrence for $\beta = 0$. Right panel: lifetime for $\beta = 10^{-3}$. The enhancement is robust for states where the measured qubits are initially in different states. The lifetime axis in the right panel is shown on a logarithmic scale to accommodate the large value $\tau = 3000$ obtained for the $|1001\rangle$ state alongside the much shorter lifetimes of the other states.

7 Discussion and Conclusion

We have shown that an asymmetric coherent drive applied to a single qubit in a collectively dissipating multi-qubit system can preserve and, for $n \geq 4$, enhance the steady-state concurrence between the undriven qubits. The enhancement reaches about 17% for $n = 4$ and persists with a gradual decrease for larger n. An approximate analytical model based on adiabatic elimination provides a qualitative explanation of the effect and predicts a $C_\infty \sim 1/n$ scaling in the range studied.

In the presence of local dephasing, the steady-state concurrence vanishes for any $\beta > 0$, but the peak concurrence is still enhanced by the drive, at the cost of a $\sim 20\%$ reduction in the lifetime. The initial-state dependence reveals that the enhancement is specific to configurations where the qubits of interest are initially in different states, but within that class, the effect is robust.

These findings may be relevant for experimental realizations with superconducting qubits in circuit QED architectures, where individual addressing is available [9, 10, 19]. The simplicity of the protocol—a single resonant drive—makes it attractive for implementation. Future work could extend the analysis to finite temperatures, non-Markovian effects, or other entanglement measures such as the logarithmic negativity. It would also

be interesting to explore whether the enhancement can be further optimized by using pulse-shaping techniques or by considering different coupling geometries.

Data Availability

All Python code implementing the Lindblad master equation simulations, including collective dissipation, asymmetric driving, and concurrence calculations, is openly available at https://github.com/atiye1995/asymmetric-driving-entanglement. All numerical results for the figures and tables can be reproduced using the provided scripts.

Acknowledgments

The authors would like to express their gratitude to the Department of Physics at Shahed University for providing the necessary resources and computational support for this research. We also thank our colleagues for their insightful discussions and feedback, which greatly contributed to the development of this work.

References

[1] R. Horodecki, P. Horodecki, M. Horodecki, and K. Horodecki, Rev. Mod. Phys. **81**, 865 (2009).

[2] M. A. Nielsen and I. L. Chuang, *Quantum Computation and Quantum Information* (Cambridge University Press, 2000).

[3] H.-P. Breuer and F. Petruccione, *The Theory of Open Quantum Systems* (Oxford University Press, 2002).

[4] C. W. Gardiner and P. Zoller, *Quantum Noise* (Springer, 2004).

[5] D. A. Lidar, Adv. Chem. Phys. **154**, 295 (2014).

[6] S. Diehl, A. Micheli, A. Kantian, B. Kraus, H. P. Büchler, and P. Zoller, Nature Phys. **4**, 878 (2008).

[7] B. Kraus, H. P. Büchler, S. Diehl, A. Kantian, A. Micheli, and P. Zoller, Phys. Rev. A **78**, 042307 (2008).

[8] F. Verstraete, M. M. Wolf, and J. I. Cirac, Nature Phys. **5**, 633 (2009).

[9] A. Wallraff, D. I. Schuster, A. Blais, L. Frunzio, R.-S. Huang, J. Majer, S. Kumar, S. M. Girvin, and R. J. Schoelkopf, Nature **431**, 162 (2004).

[10] A. Blais, A. L. Grimsmo, S. M. Girvin, and A. Wallraff, Rev. Mod. Phys. **93**, 025005 (2021).

[11] D. Leibfried, R. Blatt, C. Monroe, and D. Wineland, Rev. Mod. Phys. **75**, 281 (2003).

[12] L. Memarzadeh and S. Mancini, Phys. Rev. A **87**, 032303 (2013).

[13] W. K. Wootters, Phys. Rev. Lett. **80**, 2245 (1998).

[14] M. B. Plenio and S. F. Huelga, Phys. Rev. Lett. **88**, 197901 (2002).

[15] P. Rebentrost, R. Chakrabarti, M. Allen, and A. Aspuru-Guzik, New J. Phys. **11**, 033003 (2009).

[16] M. J. Kastoryano, F. Reiter, and A. S. Sørensen, Phys. Rev. Lett. **106**, 090502 (2011).

[17] F. Reiter and A. S. Sørensen, Phys. Rev. A **85**, 032111 (2012).

[18] Y. Lin, J. P. Gaebler, F. Reiter, T. R. Tan, R. Bowler, A. S. Sørensen, D. Leibfried, and D. J. Wineland, Nature **504**, 415 (2013).

[19] M. Kjaergaard, M. E. Schwartz, J. Braumüller, P. Krantz, J. I.-J. Wang, S. Gustavsson, and W. D. Oliver, Annu. Rev. Condens. Matter Phys. **11**, 369 (2020).

[20] H. J. Carmichael, *Statistical Methods in Quantum Optics 1* (Springer, 1999).

Author Contributions

A.Z. performed the numerical simulations, generated all figures and tables, and wrote the initial draft. Z.B. conceptualized the research direction, supervised the project, validated the results, provided critical feedback, and edited the final version. Both authors reviewed and approved the final version.

Corresponding Author

Correspondence to Zahra Bakhshi (z.bakhshi@shahed.ac.ir).

Competing Interests

The authors declare no competing interests.

Funding

The authors declare no funding agency supports this research.